Acrylamide induces human chondrocyte cell death by initiating autophagy-dependent ferroptosis

HUI WANG[1], ZIZHENG TANG[1], SHASHA LIU[1], KANGQI XIE[1] and HUA ZHANG[2]

[1]Department of Rheumatology, The Fourth Hospital of Jinan, Jinan, Shandong 250031; [2]Department of Rheumatology, Zaozhuang Municipal Hospital (Affiliated Hospital of Jining Medical College), Zaozhuang, Shandong 277102, P.R. China

Received June 29, 2022; Accepted February 8, 2023

DOI: 10.3892/etm.2023.11945

Abstract. Acrylamide (ACR) is formed during heat treatment of foodstuffs and ACR may serve as a probable malignant neoplastic disease agent in all organs and tissues of the human body. However, it is unknown if ACR is associated with ankylosing spondylitis (AS) pathogenesis. Cell viability and proliferation were determined using CCK-8 assay and EdU staining. Flow cytometry was used to determine cell death and cell cycle arrest. Intracellular lipid reactive oxygen species, Fe^{2+} and mitochondrial membrane potential (MMP) were analyzed using a C11-BODIPY581/591 fluorescent probe, FerroOrange staining and a JC-1 MMP Assay kit, respectively. The present study showed that ACR decreased chondrocyte cell viability in a dose-dependent manner and that ACR significantly promoted chondrocyte senescence. ACR also elevated the expression of cell cycle arrest-associated proteins, including p53, cyclin-dependent kinase inhibitor 1 and cyclin-dependent kinase inhibitor protein, in human chondrocytes. Similarly, DNA damage was also enhanced following ACR treatment in chondrocytes. In addition, the ferroptosis-specific inhibitor ferrostatin-1 (Fer-1) and the autophagy inhibitor 3-methyl-adenine abolished ACR-induced cell death in chondrocytes. ACR was shown to activate autophagic flux and induce mitochondrial dysfunction by increasing the MMP. Western blot analysis of ferroptosis-related proteins demonstrated that ACR decreased the expression of glutathione peroxidase 4, solute carrier family 7 member 11, transferrin receptor protein 1 and ferritin heavy chain 1 in chondrocytes whereas Fer-1 abolished these effects. ACR treatment significantly elevated the phosphorylation levels of AMP-activated protein kinase (AMPK) and serine/threonine-protein kinase ULK1 in human chondrocytes. Notably, the effect of ACR was diminished by knockdown of AMPK, as evidenced by reduced lipid reactive oxygen species accumulation and Fe^{2+} levels. Hence, ACR inhibited cell proliferation and contributed to cell death by inducing autophagy-dependent ferroptosis while promoting autophagy by activating AMPK-ULK1-mTOR signaling in human chondrocytes. It was hypothesized that the presence of ACR in foodstuffs may increase the risk of AS and that decreasing ACR in food products is of importance.

Correspondence to: Dr Hua Zhang, Department of Rheumatology, Zaozhuang Municipal Hospital (Affiliated Hospital of Jining Medical College), 41 Longtou Middle Road, Shizhong, Zaozhuang, Shandong 277102, P.R. China
E-mail: zhabghua0303@sina.com

Key words: acrylamide, ankylosing spondylitis, autophagy, ferroptosis, AMPK/ULK1/mTOR signaling

Introduction

Ankylosing spondylitis (AS) is a chronic autoimmune inflammatory disease that primarily invades the spine and involves the cuboid iliac joint (1). The disability rate of patients with AS is high and AS has a serious impact on quality of life (2,3). Studies have shown that AS is associated with genetics, infection, immunity, inflammatory cell infiltration, cytokine imbalance and other factors (4,5).

In the ligaments of patients with early AS, increased chondrocyte differentiation promotes cartilage formation, which is accompanied by cartilage calcification Chen *et al* (4) found that long non-coding RNA metastasis-associated lung adenocarcinoma transcript 1 and gasdermin-D expression is increased in AS cartilage tissue and chondrocytes, whereas microRNA-558 expression is decreased in AS chondrocytes, thereby promoting chondrocyte pyroptosis and activating the inflammatory response *in vivo* (4,5). Moreover, one of the hallmarks of AS joint remodeling is cartilage degeneration and increased chondrocyte apoptosis (6). The aforementioned studies suggest that chondrocyte death accelerates cartilage degeneration and promotes the disease course of AS.

Ferroptosis is a cell death pathway that is distinct from apoptosis, necrosis and autophagy at the biochemical, morphological and genetic levels (7). Several studies confirmed that excessive autophagy could promote ferroptosis (8-10). In immortalized mouse embryonic fibroblasts, PANC1 and PANC2.03 human pancreatic cancer cell lines as well as human fibrosarcoma cell line HT-1080, knockdown of autophagy-related 5 and autophagy-related 7 inhibits autophagy and levels of intracellular free iron levels and lipid peroxidation end products [such as malondialdehyde (MDA)] decrease significantly (9,11). Moreover, expression of ferritin heavy chain 1 (FTH1), an intracellular ferritin marker, is significantly increased (9,11). In addition, autophagy is

accompanied by a decrease in glutathione under conditions such as starvation of fetal bovine serum (FBS) and oxidative stress (12). By contrast, glutathione peroxidase 4 (GPX4) overexpression inhibits reactive oxygen species (ROS)-mediated autophagy (13). Other ferroptosis regulators such as solute carrier family 7 member 11 (SLC7A11) have also been shown to be potential regulators of autophagy (14). Through weighted gene co-expression network analysis, Rong *et al* (13) demonstrated that ferroptosis-associated gene expression is abnormal, e.g., that of small nucleolar RNA host gene 16 and mitogen-activated protein kinase 1, in patients with AS, leading to the speculation that ferroptosis is involved in the pathological development of AS.

Acrylamide (ACR) is a synthetic compound utilized commercially and is also a cytotoxic and genotoxic compound that forms during heat treatment of foodstuffs, such as potatoes, bakery products and plant derivatives, as a β-unsaturated (conjugated) reactive molecule (15). Increasing studies have suggested ACR as a probable malignant neoplastic disease agent in all organs and tissues of the human body (16,17). For example, ACR induces human chondrocyte death by mitochondrial dysfunction (15). However, to the best of our knowledge, if ACR contributes to AS pathogenesis via ferroptosis remains unclear.

Materials and methods

Cell culture. Human chondrocytes were purchased from Procell Life Science & Technology Co., Ltd. (cat. no. CP-H107). Chondrocytes were cultured in human chondrocyte complete culture medium (cat. no. CM-H107; Procell Life Science & Technology Co., Ltd.) supplemented with 10% FBS (Invitrogen; Thermo Fisher Scientific, Inc.), streptomycin (100 mg/ml) and penicillin (100 U/ml) at 37˚C in a humidified atmosphere with 5% CO_2. Human chondrocytes were treated with ACR (ACR group; cat. no. V900845; Sigma-Aldrich; Merck KGaA) or an equal volume of sterilized water (Con group) for 24 h at 37˚C.

Cell counting kit (CCK)-8 assay. Human chondrocytes were seeded into a 96-well plate at a density of 5.0×10^3 cells/well. Following exposure to 0.1, 0.2, 0.4, 0.8, 1.6, 3.2 or 6.4 μg/ml ACR for 24 h at 37˚C, chondrocyte viability was determined using a CCK-8 assay kit (Beijing Solarbio Science & Technology Co., Ltd.) according to the manufacturer's instructions. In brief, human chondrocytes were incubated with 10 μl CCK-8 regent at 37˚C for 1 h. Next, cell viability was calculated from the optical density measured at 450 nm using a microplate reader and PBS without any cells was used as a blank control (Thermo Fisher Scientific, Inc.). The half-maximal inhibitory concentration (IC_{50}) values were calculated via the Reed-Muench method (18).

Human chondrocytes were also seeded in a 96-well plate at a density of 5,000 cells/well. To validate which type of cell death could be induced by ACR, human chondrocytes were preincubated with ferrostatin-1 (Fer-1) (1 μM; a ferroptosis inhibitor), benzyloxycarbonylvalyl-alanyl-aspartyl fluoromethyl ketone (Z-VAD-FMK) (20 μM; a caspase-3 inhibitor), necrostatin-1 (Nec-1) (20 μM; a necroptosis inhibitor) and 3-MA (20 μM; an autophagy inhibitor) for 1 h. The human chondrocytes were then further treated with 0.35 μg/ml ACR at 37˚C for 24 h. Chondrocyte viability was determined using a CCK-8 assay kit (Beijing Solarbio Science & Technology Co., Ltd.) according to the manufacturer's instructions. The absorbance values were determined at OD450 nm using a microplate reader (Thermo Fisher Scientific, Inc.). Dead cells (%)=100-OD experimental group/OD control group x100.

EdU staining. Human chondrocytes were seeded in a 96-well plate at a density of 5.0×10^3 cells/well and treated with 0.35 μg/ml ACR for 24 h at 37˚C. EdU-positive cells were stained with a Cell-Light™ EdU Apollo *In Vitro* kit (Guangzhou RiboBio Co., Ltd.) according to the manufacturer's instructions. A total of 100 μl of 50 μM EdU medium was added to each well and incubated at 37˚C for 2 h. The medium was then discarded. Afterwards, the cells were washed twice with PBS for 5 min each time. Next, 100 μl 4% paraformaldehyde (Beijing Solarbio Science & Technology Co., Ltd.) was added to each well and incubated for 30 min at room temperature, and 100 μl of 1X DAPI (cat. no. LI-9557; OriGene Technologies, Inc.) was added to each well and incubated for 30 min at room temperature, avoiding light and then discarded. Once the staining reaction solution was discarded, 100 μl PBS was added to each well. After washing three times, the slides were observed under a fluorescence microscope (Keyence Corporation).

EdU is a thymidine nucleoside analogue that is incorporated into replicating DNA molecules instead of thymine during cell proliferation and rapidly labels the replication activity of DNA in cells by the specific reaction of EdU with fluorescent dyes (19). EdU-positive cells indicate active replication.

Senescence-associated β-galactosidase staining. Human chondrocytes were seeded into a six-well plate at a density of 1×10^6 cells/well and treated with 0.35 μg/ml ACR for 24 h at 37˚C. Subsequently, chondrocytes were stained with Senescence β-Galactosidase Staining kit (cat. no. C0602; Beyotime Institute of Biotechnology) according to the manufacturer's instructions. In brief, cells were fixed with 4% paraformaldehyde (Beyotime Institute of Biotechnology) for 10 min at room temperature. The cells were washed three times with PBS (5 min/time). After that, the PBS was discarded, and 1 ml β-gal staining solution (cat. no. C0602; Beyotime Institute of Biotechnology) was added to each well and incubated at 37˚C for 1 h followed by three washes with PBS (5 min/time). Aging cells were observed under a light microscope and determined by counting the number of blue-stained cells. The cytoplasm of β-galactosidase-containing cells was blue or dark blue. A total of five fields of view were randomly selected from each section, the number of blue or dark blue cells was counted manually, and the average was taken for statistical analysis.

Immunofluorescence (IF) staining. Human chondrocytes (1×10^6 cells/well) were seeded on coverslips, fixed with 4% paraformaldehyde (Beyotime Institute of Biotechnology) at room temperature for 10 min and permeabilized with 1% Triton X-100 (Beyotime Institute of Biotechnology) for 15 min at room temperature. Slides were blocked with 8% BSA (Beijing Solarbio Science & Technology Co., Ltd.) at room temperature for 2 h and then incubated with γ-H2A histone family member

X primary antibody (γ-H2AX; cat. no. C2035S; 1;100; DNA Damage Assay kit; Beyotime Institute of Biotechnology) or anti-AMP-activated protein kinase primary antibody (cat. no. 5832, anti-AMPK; 1:50; CST Biological Reagents Co., Ltd.) at 4˚C overnight. Then, slides were incubated with FITC-conjugated secondary antibody (cat. no. ZF-0314; OriGene Technologies, Inc.) at room temperature for 2 h in the dark and mounted with fluorescent mounting medium with DAPI (cat. no. LI-9557; OriGene Technologies, Inc.). The slides were observed under a light microscope (Keyence Corporation). The density of relative fluorescence intensity was analyzed using ImageJ 1.43b software (National Institutes of Health).

Western blotting. Human chondrocytes ($2x10^6$ cells in total for each sample) were lysed with RIPA buffer (cat. no. R0010, Beijing Solarbio Science & Technology Co., Ltd.) containing protease and phosphatase inhibitors (Sigma-Aldrich; Merck KGaA) for 30 min on ice. The lysates were centrifuged at 11,000 x g for 30 min at 4˚C and protein concentration was determined using a BCA Protein Assay kit (Pierce; Thermo Fisher Scientific, Inc.). Equal amounts of proteins (20 μg/lane) were isolated by SDS-PAGE on a 12% gel and transferred onto polyvinylidene fluoride membranes (MilliporeSigma). The membranes were blocked with 6% non-fat milk (MilliporeSigma) at room temperature for 2 h and incubated with primary antibodies as follows: p53 (cat. no. 2527; 1:1,000), cyclin-dependent kinase inhibitor 1 (p21; cat. no. 2947; 1:1,000), cyclin-dependent kinase inhibitor protein (p16; cat. no. 80772; 1:1,000), light chain (LC) 3I/II (cat. no. 3868; 1:1,000), sequestosome 1 (p62; cat. no. 88588; 1:1,000), GPX4 (cat. no. 59735, 1:1,000), SLC7A11 (cat. no. 12691; 1:1,000; SLC7A11); transferrin receptor protein 1 (TfR1; cat. no. 13113; 1:1,000; SLC7A11), FTH1 (cat. no. 4393, 1:1,000), AMPK (cat. no. 5832, 1:1,000), phosphorylated (p)-AMPK (cat. no. 2537, 1:1,000), serine/threonine-protein kinase ULK1 (cat. no. 8054, 1:1,000), p-ULK1 (cat. no. 14202, 1:1,000), p-mTOR (cat. no. 5536, 1:1,000); mTOR (cat. no. 2983, 1:1,000) and GAPDH (cat. no. 5174, 1:1,000) (all CST Biological Reagents Co., Ltd.) at 4˚C overnight. After washing with PBST (0.1% Tween-20 in PBS; Beijing Solarbio Science & Technology Co., Ltd.) three times, membranes were incubated with horseradish peroxidase (HRP)-conjugated goat anti-rabbit IgG (cat. no. ZB-2301; 1:5,000; OriGene Technologies, Inc.) for 2 h at room temperature. The protein signal was determined using Immobilon Western Chemiluminescent HRP Substrate (cat. no. WBKLS0500; MilliporeSigma). Relative protein expression was normalized to that of GAPDH. The density of each band was analyzed using ImageJ 1.43b software (National Institutes of Health).

Knockdown of AMPK. Specific small interfering (si)RNA targeting AMPK (siRNA-AMPK; 5'-AAAGTGAAGGTT GGCAAACATGA-3') or negative control (NC; 5'-CCGAUA GGUUUACUGCCAATT-3') was purchased from Guangzhou RiboBio Co., Ltd. and transfected using HiperFect Transfection Reagent (Qiagen GmbH) according to the manufacturer's instructions, and subsequent experiment was performed after 48 h of transfection. In brief, human chondrocytes were seeded into a six-well plate at a density of $1x10^6$ cells/well for 24 h and then 10 μl HiperFect Transfection Reagent was mixed with 100 μl serum-free culture medium. Subsequently, 4 μl siRNA-AMPK (10 μM) or NC (10 μM) was added and it was incubated at room temperature for 10 min. Subsequently, the mixture was added to each well of a six-well plate at a final concentration of 20 nM and incubated at 37˚C for 24 h before cells were collected for further study.

Determination of lipid ROS. Human chondrocytes were seeded into a 6-well plate at a density of $1x10^6$ cells/well and lipid ROS levels were determined following incubation with 5 μM C11-BODIPY581/591 fluorescent probe (MedChemExpress) for 20 min at 37˚C in the dark. Then, fluorescence was observed under a light microscope (Keyence Corporation).

Mitochondrial membrane potential (MMP) evaluation. MMP was determined using the JC-1 MMP Assay kit (cat. no. ab113850; Abcam) according to the manufacturer's instructions. Human chondrocytes were seeded into a six-well plate at a density of $1x10^6$ cells/well and treated with 0.35 μg/ml ACR for 24 h at 37˚C. Subsequently, cells were incubated with 1X JC-1 staining solution for 20 min in the dark at 37˚C and observed under a fluorescence microscope (Keyence Corporation). Normal MMP was shown in red with JC-1 dimers whereas depolarized membrane potential was shown in green with JC-1 monomers.

Determination of intracellular Fe^{2+} levels. Human chondrocytes were stained with 1 μM FerroOrange (Dojindo Laboratories, Inc.) in Hanks' balanced salt solution (cat. no. H1045; Beijing Solarbio Science & Technology Co., Ltd.) at 37˚C for 30 min in the dark and immediately observed under a fluorescence microscope (Keyence Corporation).

Determination of ROS and MDA levels. ROS and MDA content were measured using a ROS Assay kit (cat. no. S0033S; Beyotime Institute of Biotechnology) and Lipid Peroxidation MDA Assay kit (cat. no. S0131S; Beyotime Institute of Biotechnology), respectively, according to the manufacturer's instructions. Human chondrocytes were seeded into a 6-well plate at a density of $1x10^6$ cells/well and were treated with 0.35 μg/ml ACR for 24 h at 37˚C. After that, the cells were collected for further determination of intracellular ROS and MDA contents.

For ROS quantification, human chondrocytes were incubated with 10 μM DCFH-DA for 20 min at 37˚C in the dark and immediately observed under a fluorescence microscope (Keyence Corporation). The density of relative fluorescence intensity was analyzed using ImageJ 1.43b software (National Institutes of Health).

For MDA quantification, 0.1 ml of sample or PBS (blank control) was added to the centrifuge tube, followed by 0.2 ml of MDA assay working solution. The mixture was heated at 100˚C for 15 min. The water bath was cooled to room temperature and centrifuged at 1,000 x g for 10 min at room temperature. After that, 200 μl of supernatant was added to a 96-well plate, followed by determination of absorbance at 532 nm using a microplate reader (Thermo Fisher Scientific, Inc.). The relative MDA content in the sample solution was calculated from the standard curve.

Transmission electron microscopy. Human chondrocytes were fixed in 2.5% glutaraldehyde solution at room temperature for 2 h, post-fixed in 1% aqueous osmium tetroxide at room temperature for 2 h and dehydrated in an ethanol gradient (50, 70 and 90%) at room temperature for 15 min separately and 100% acetone at room temperature for 15 min. The samples were prepared by gradient infiltration of anhydrous acetone and epoxy resin overnight, embedded in resin and polymerized at 60˚C for 48 h. The samples were cut into 50 nm ultrathin sections using an ultramicrotome (Leica Microsystems GmbH), stained with 3% uranium acetate-lead citrate (Beijing Zhongxing Bairui Technology Co., Ltd.) at room temperature for 15 min and examined by 120 keV transmission electron microscopy (Tecnai G2 20 TWIN; Thermo Fisher Scientific, Inc.).

Flow cytometry analysis. Human chondrocytes were seeded into a six-well plate at a density of $1x10^6$ cells/well and treated with 0.35 μg/ml ACR for 24 h at 37˚C. Subsequently, the cells were collected for cell death and cell cycle analysis using an Annexin V-PE/7-AAD Apoptosis Detection (cat. no. 40310ES50; Shanghai Yeasen Biotechnology Co., Ltd.) and Cell Cycle Assay Kit (Red Fluorescence; E-CK-A351; Elabscience Biotechnology Co., Ltd.) according to the manufacturer's instructions.

The cells were centrifuged at 300 x g at 4˚C for 5 min to collect the cells. The cells were washed twice with PBS precooled at 4˚C and centrifuged at 300 x g at 4˚C for 5 min. Subsequently, 250 μl 1X binding buffer was added to resuspend the cells and the concentration was adjusted to $1x10^6$ cells/ml. Then, 100 μl cell suspension was transferred into a 5 ml flow tube and incubated with 5 μl annexin V/PE and 10 μl 7-AAD in the dark at room temperature for 15 min. The cells were tested within 1 h using a flow cytometer (BD LSRFortessa™; BD Biosciences). The data was analyzed using FlowJo 10.8.1 software (FlowJo LLC).

Approximately $5x10^5$ human chondrocytes were collected. The cells were centrifuged at 300 x g for 5 min and the supernatant was discarded. Next, 0.3 ml PBS was added to resuspend the cells. Afterwards, 1.2 ml of-20˚C anhydrous ethanol was added, mixed thoroughly and the samples were placed at -20˚C for 1 h. Next, the samples were centrifuged at 300 x g for 5 min, the supernatant was discarded and 1 ml PBS was added to resuspend the cells for 15 min at room temperature. Afterwards, the mixture was centrifuged at 300 x g for 5 min, the supernatant was discarded and 100 μl of RNase A was added. Finally, 400 μl PI Reagent (50 μg/ml) was added and mixed through thoroughly, and the cells were incubated for 30 min at 4˚C under low light. The red fluorescence at 488 nm was recorded immediately on a BD LSRFortessa flow cytometer (BD Biosciences). The data was analyzed using FlowJo 10.8.1 software (FlowJo LLC).

Determination of autophagic flux. Human chondrocytes were seeded into a six-well plate at a density of $1x10^6$ cells/well and were transfected with GFP-mCherry-LC3 adenovirus at 100 multiplicity of infection (MOI) for 24 h at 37˚C. Following treatment with 0.35 μg/ml ACR for 24 h at 37˚C, cells were fixed with 4% paraformaldehyde (Beyotime Institute of Biotechnology) at room temperature for 10 min and immediately observed under a microscope (Keyence Corporation). GFP degraded in the acidic environment. After the red-green fluorescence was merged, the yellow spots that appeared after the merge were only autophagosomes. The red spots indicated autolysosomes. If the autophagic flow was unblocked, the red fluorescence was more than the yellow fluorescence. If the autophagic flow was blocked, it was mainly yellow fluorescence. Autophagic flux was determined by counting the cells with GFP+/mCherry+ (yellow) or GFP-/mCherry+ (red) puncta manually using a fluorescence microscope (Keyence Corporation).

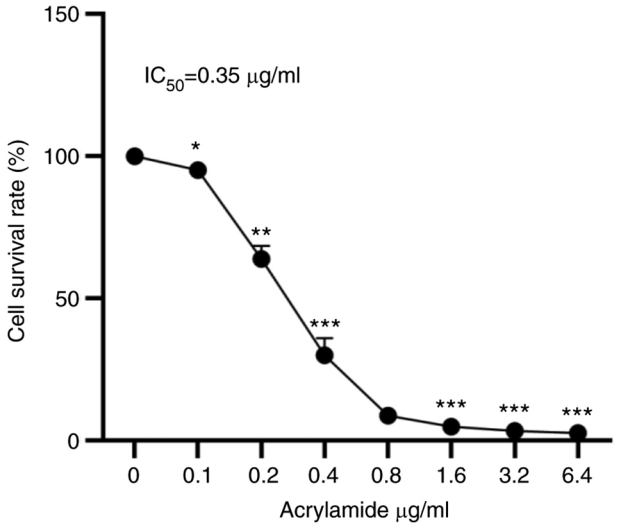

Figure 1. Cell Counting Kit-8 assay determination of IC_{50} of acrylamide in human chondrocytes. *P<0.05, **P<0.01; ***P<0.001 vs. 0 μg/ml ACR. IC_{50}, half maximal inhibitory concentration.

Statistical analysis. The data are expressed as the mean ± standard deviation of three independent experimental repeats. Unpaired Student's t test was used for comparisons between two groups. Comparisons between three or more groups were performed via one-way ANOVA followed by Bonferroni's post hoc test. All analyses were performed using GraphPad Prism 8 statistical software (GraphPad Software, Inc.). P<0.05 was considered to indicate a statistically significant difference.

Results

ACR decreases human chondrocyte survival rate in a dose-dependent manner. To analyze the effects of ACR on human chondrocyte viability, cells were treated with ACR at 0.1, 0.2, 0.4, 0.8, 1.6, 3.2 and 6.4 μg/ml ACR for 24 h. Compared with the control, the cell survival rate of human chondrocytes decreased significantly in a dose-dependent manner (P<0.05; Fig. 1). The IC_{50} of ACR in human chondrocytes was 0.35 μg/ml.

ACR suppresses chondrocyte proliferation. To determine the effect of ACR on cell proliferation, human chondrocytes were incubated with 0.35 μg/ml ACR at 37˚C for 24 h and EdU staining was performed. EdU-positive cells/field were significantly decreased in chondrocytes treated with ACR compared with Con chondrocytes (P<0.001; Fig. 2A). In addition, cell

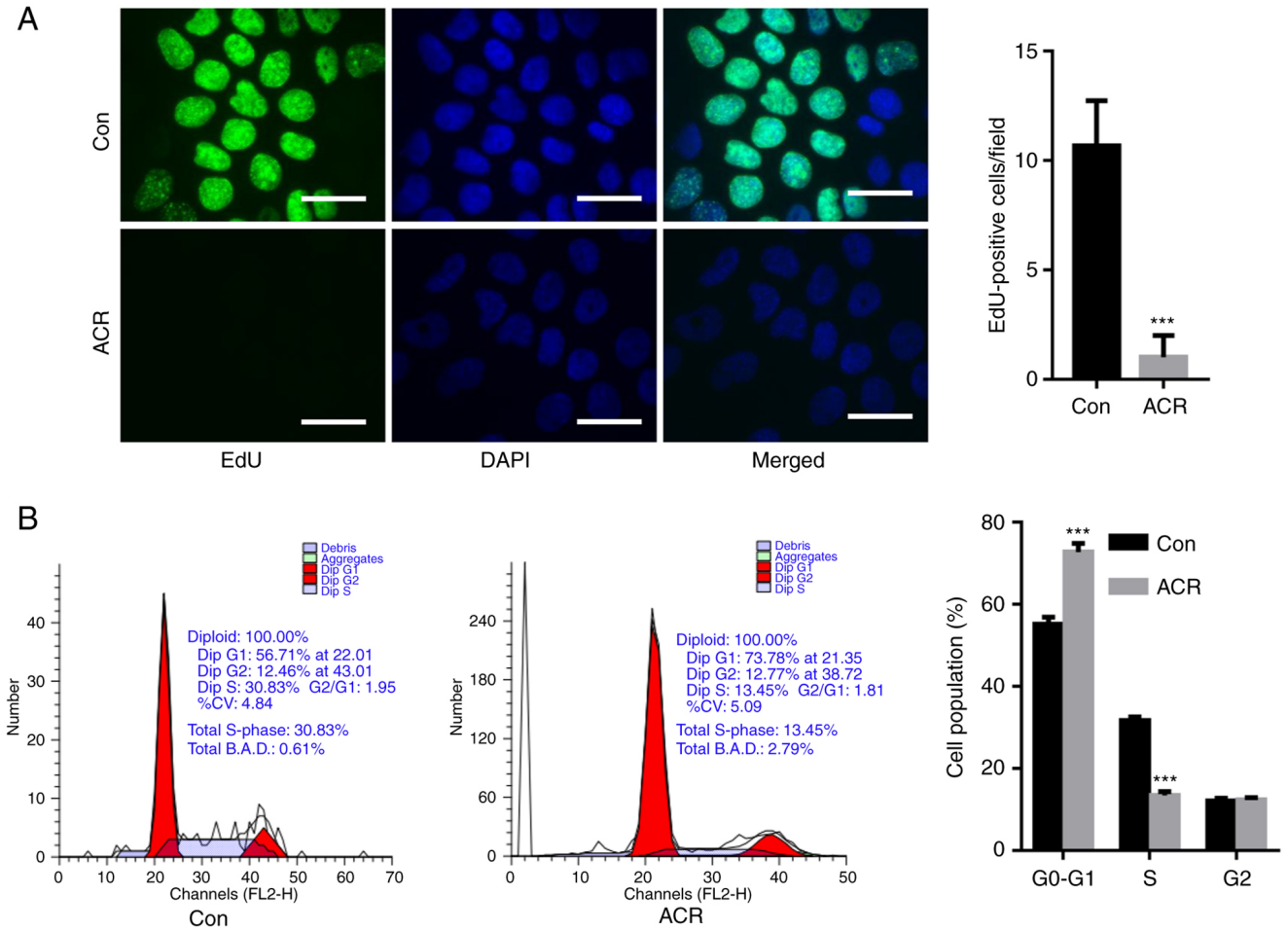

Figure 2. ACR suppresses chondrocyte proliferation. (A) EdU staining showed that ACR decreased the number of EdU-positive cells in human chondrocytes (magnification, x20; scale bar, 30 μm). (B) Flow cytometry analysis showed that ACR induced cell cycle arrest in human chondrocytes. ***P<0.001 vs. Con. ACR, acrylamide; Con, control.

cycle arrest was observed in human chondrocytes treated with ACR, as evidenced by elevation in the G_0-G_1 phase cell population and downregulation of the S phase cell population compared with Con (P<0.001; Fig. 2B).

ACR induces human chondrocyte senescence. Compared with Con, 0.35 μg/ml ACR significantly increased the number of SA-β-gal-positive cells after 24 h (P<0.001; Fig. 3A). In addition, relative fluorescence of γ-H2AX (a biomarker of DNA damage) was increased in human chondrocytes treated with ACR compared with Con (Fig. 3B). Moreover, flow cytometry analysis showed that ACR increased the number of dead cells to ~28% compared with that of Con (11%; P<0.001; Fig. 3C). Western blotting showed that the expression levels of cell arrest-associated proteins, including p53, p21 and p16, were significantly enhanced in human chondrocytes treated with ACR compared with those in Con chondrocytes (P<0.05; Fig. 3D). These observations indicated that ACR contributed to the senescence of human chondrocytes.

Ferrostatin-1 (Fer-1) and 3-methyladenine (3-MA) reverse ACR-induced cell death in human chondrocytes. It was investigated whether 0.35 μg/ml ACR decreased human chondrocyte cell death in a time-dependent manner. CCK-8 assay showed that cell viability was significantly decreased in human chondrocytes treated with 0.35 μg/ml ACR at 24, 48 and 72 h (P<0.01; Fig. 4A). To validate which type of cell death was induced by ACR, human chondrocytes were preincubated with Fer-1, Z-VAD-FMK, Nec-1 and 3-MA for 1 h. Human chondrocytes were further treated with 0.35 μg/ml ACR at 37˚C for 24 h. Fer-1 and 3-MA significantly reversed ACR-induced cell death (P<0.01; Fig. 4B). These findings demonstrated that ACR promoted chondrocyte cell death by inducing ferroptosis and autophagy.

ACR induces autophagy in human chondrocytes. Ultrastructural analysis indicated a higher level of outer mitochondrial membrane rupture in chondrocytes treated with 0.35 μg/ml ACR at 37˚C for 24 h compared with that in Con chondrocytes (Fig. 5A). Meanwhile, the mitochondrial ridge was decreased or disappeared in human chondrocytes treated with ACR (Fig. 5A). By contrast, preincubation with 3-MA at 37˚C for 1 h reversed these effects (Fig. 5A). Autophagic flux was activated in human chondrocytes treated with ACR, as evidenced by the elevation in red puncta, whereas 3-MA preincubation significantly decreased the red puncta in human chondrocytes (P<0.001; Fig. 5B). Western blotting of autophagic flux showed that the LC3II/LC3I ratio

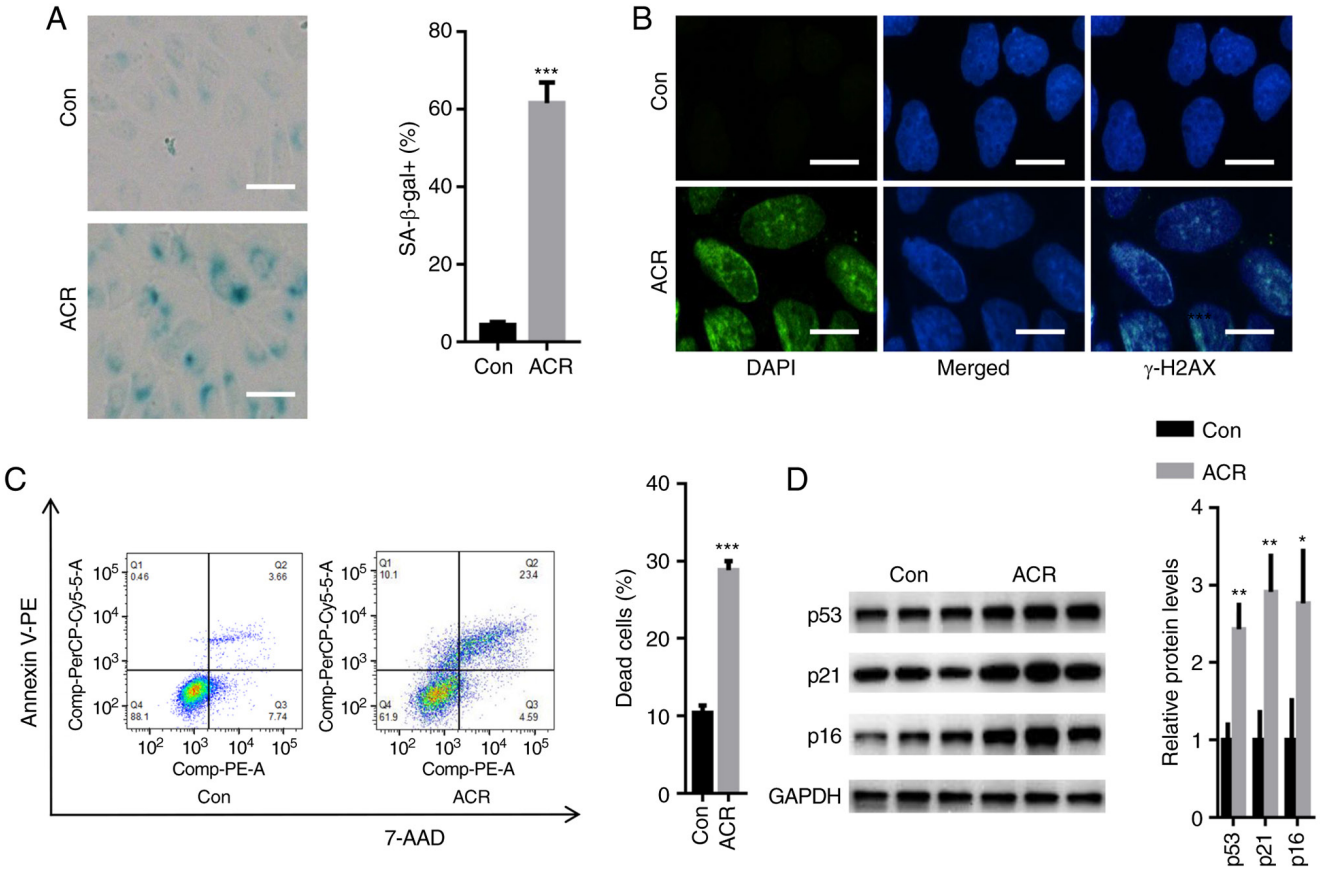

Figure 3. ACR induces human chondrocyte senescence. (A) SA-β-gal staining showed that 0.35 μg/ml ACR significantly increased the number of SA-β-gal-positive cells (magnification, x20; scale bar, 20 μm). (B) Immunofluorescence staining showed that the relative fluorescence of γ-H2A histone family member X was increased in human chondrocytes treated with ACR (magnification, x40; scale bar, 10 μm). (C) Flow cytometry showed that ACR increased the number of dead cells. (D) Western blot assay showed that expression levels of p53, cyclin-dependent kinase inhibitor 1 and cyclin-dependent kinase inhibitor protein were significantly increased in human chondrocytes treated with ACR. *P<0.05, **P<0.01 and ***P<0.001 vs. Con. ACR, acrylamide; Con, control; SA-β-gal, senescence-associated β-galactosidase; γ-H2AX, γ-H2A histone family member X.

was increased, whereas expression of p62 was decreased in human chondrocytes treated with ACR (P<0.01; Fig. 5C). By contrast, 3-MA preincubation decreased the LC3II/LC3I ratio and increased the protein expression of p62 compared with the ACR treatment alone (P<0.01; Fig. 5C). These results indicate that ACR activated autophagic flux in human chondrocytes.

ACR promotes ferroptosis in human chondrocytes. Changes in mitochondrial function are a hallmark of ferroptosis (20). Hence, cellular MMP was evaluated in human chondrocytes treated with 0.35 μg/ml ACR at 37˚C for 24 h. When human chondrocytes were treated with ACR, poly JC-1 molecules were dissociated into mono JC-1 molecules, suggesting a reduction or loss of MMP (Fig. 6A). In the Fer-1 group, poly JC-1 was enhanced whereas mono JC-1 was decreased in human chondrocytes (Fig. 6A). FerroOrange staining showed an increase in red fluorescence density after ACR treatment whereas Fer-1 preincubation decreased the red fluorescence density in chondrocytes (Fig. 6B). A C11 BODIPY fluorescent probe was used to detect intracellular lipid ROS content. The data showed that ACR increased lipid-ROS accumulation in chondrocytes whereas preincubation with Fer-1 decreased intracellular lipid-ROS levels (Fig. 6C). Intracellular ROS and MDA levels were investigated. Fer-1 attenuated ACR-induced upregulation of ROS and MDA contents (P<0.01; Fig. 6D). Western blotting of ferroptosis-associated proteins demonstrated that ACR reduced expression of GPX4, SLC7A11, TfR1 and FTH1 in chondrocytes whereas Fer-1 abolished these effects (P<0.05; Fig. 6E). These observations indicated that ACR induced chondrocyte ferroptosis.

ACR activates AMPK/ULK1 signaling in human chondrocytes. Some studies have demonstrated an important role of AMPK/ULK1 in autophagy and ferroptosis (21,22); thus, the present study investigated the effects of ACR on AMPK signaling. ACR increased the phosphorylation of AMPK and ULK1 but suppressed activation of mTOR in human chondrocytes at 24 and 48 h (P<0.05: Fig. 7A). To elucidate if ACR induced autophagy and ferroptosis by activating AMPK signaling, a specific siRNA targeting AMPK was used. Western blotting showed that transfection with siRNA AMPK significantly reduced expression of AMPK compared with NC (Fig. 7B). IF staining showed that siRNA AMPK notably suppressed the fluorescence density of AMPK in human chondrocytes even in the presence of ACR (Fig. 7C). Furthermore, ACR-induced mitochondrial membrane rupture was reversed by silencing AMPK in human chondrocytes (Fig. 7D). Moreover, the upregulated levels of lipid ROS

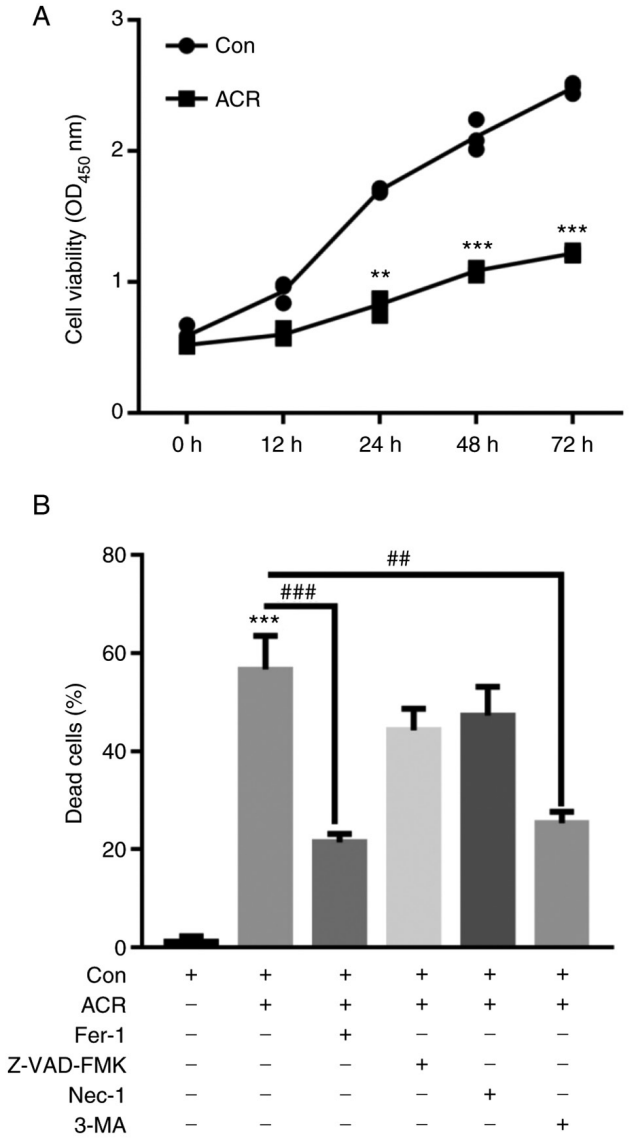

Figure 4. Fer-1 and 3-MA reverse ACR-induced cell death in human chondrocytes. (A) CCK-8 assay showed that 0.35 μg/ml ACR decreased human chondrocyte cell viability at 24, 48 and 72 h. (B) Fer-1 and 3-MA significantly reversed ACR-induced cell death. **P<0.01 and ***P<0.001 vs. Con. $^{\#\#}$P<0.01 vs. ACR and $^{\#\#\#}$P<0.001. Fer-1, ferrostatin-1; 3-MA, 3-methyladenine; ACR, acrylamide; Con, control; Nec-1, necrostatin-1; Z-VAD-MFK, benzyloxycarbonylvalyl-alanyl-aspartyl fluoromethyl ketone.

and Fe^{2+} were blocked by transfection with siRNA-AMPK (Fig. 7E and F). These data showed that ACR-induced ferroptosis and autophagy were achieved by activating AMPK/ULK1 signaling in human chondrocytes.

Discussion

In 2002, Swedish researchers demonstrated notable levels of ACR in many heat-treated carbohydrate-rich foods (23). ACR is extensively found in deep-fried sugar-rich foods, such as potato chips, bread and breakfast cereals (24). Exposure to ACR has become a public issue due to its carcinogenicity and neurotoxicity in humans (15). To the best of our knowledge, however, whether ACR is involved in the pathology of AS has not been explored.

To the best of our knowledge, the present study showed for the first time that ACR suppressed human chondrocyte proliferation in a dose-dependent manner. Moreover, ACR significantly promoted chondrocyte senescence and elevated expression of cell cycle arrest-associated proteins, including p53, p21 and p16, in human chondrocytes. Similarly, DNA damage was also enhanced following ACR treatment in chondrocytes since γ-H2AX positive cells were increased. These observations indicated a pathogenic role of ACR in human chondrocytes.

Previous studies have shown that autophagic cell death, apoptosis and necrosis are involved in the development of AS (25,26). Ferroptosis is an iron-dependent cell death pathway that is associated with pathological conditions, including osteoarthritis (27). However, whether ACR induces ferroptosis in the progression of AS remains unclear. The present study aimed to define which type of cell death could be induced by ACR in human chondrocytes and found that the ferroptosis-specific inhibitor Fer-1 and the autophagy inhibitor 3-MA abolished ACR-induced cell death in chondrocytes. Thus, it was hypothesized that ACR induced autophagic cell death and ferroptosis in human chondrocytes.

The pathological process of AS remains unclear and current treatments (e.g., sarilumab and tofacitinib) have had limited success (28,29). Recently, autophagy was described as a potential player in the pathogenesis of AS (28). Autophagy is an extremely preserved mechanism, from yeast to mammals (30). Under nutrient depletion conditions, autophagy recycles intracellular energy resources by degrading cytotoxic proteins and damaged organelles (30). However, excessive autophagy leads to aberrant cell death (30). The present study found that the levels of LC3II were increased and p62 expression was decreased by ACR treatment in human chondrocytes. ACR-induced cell autophagy was reversed by the autophagy inhibitor 3-MA. It was hypothesized speculate that ACR induced autophagy in human chondrocytes.

Ferroptosis is an autophagic cell death mode because inhibition of autophagy or knockout of autophagy-related 5 protein decreases the cytosolic labile iron pool and intracellular peroxidation (31). The present study showed that ACR induced ferroptosis in human chondrocytes via ferritinophagy. Ferritin, which contains FTH1 and ferritin light chain, acts as a key storage molecule of excess iron to maintain iron homeostasis (9). Autophagy activation degrades proteins to elevate intracellular iron levels and leads to oxidative injury via the Fenton reaction (32). Nuclear receptor coactivator 4 (NCOA4) is a selective cargo receptor for turnover of autophagic proteins in lysosomes (33). NCOA4-mediated degradation of FTH1 triggers ferroptosis (33). The present study found that expression of FTH1 was significantly suppressed by ACR in chondrocytes, indicating that iron equilibrium was disrupted by ACR, resulting in ferroptosis. In addition, ACR also decreased the protein expression of SLC7A11, a key component of the Xc-system that provides adequate concentrations of cysteine for the synthesis of glutathione, resulting in increased lipid peroxidation (34). These findings suggested induction of ferroptosis via ACR in human chondrocytes.

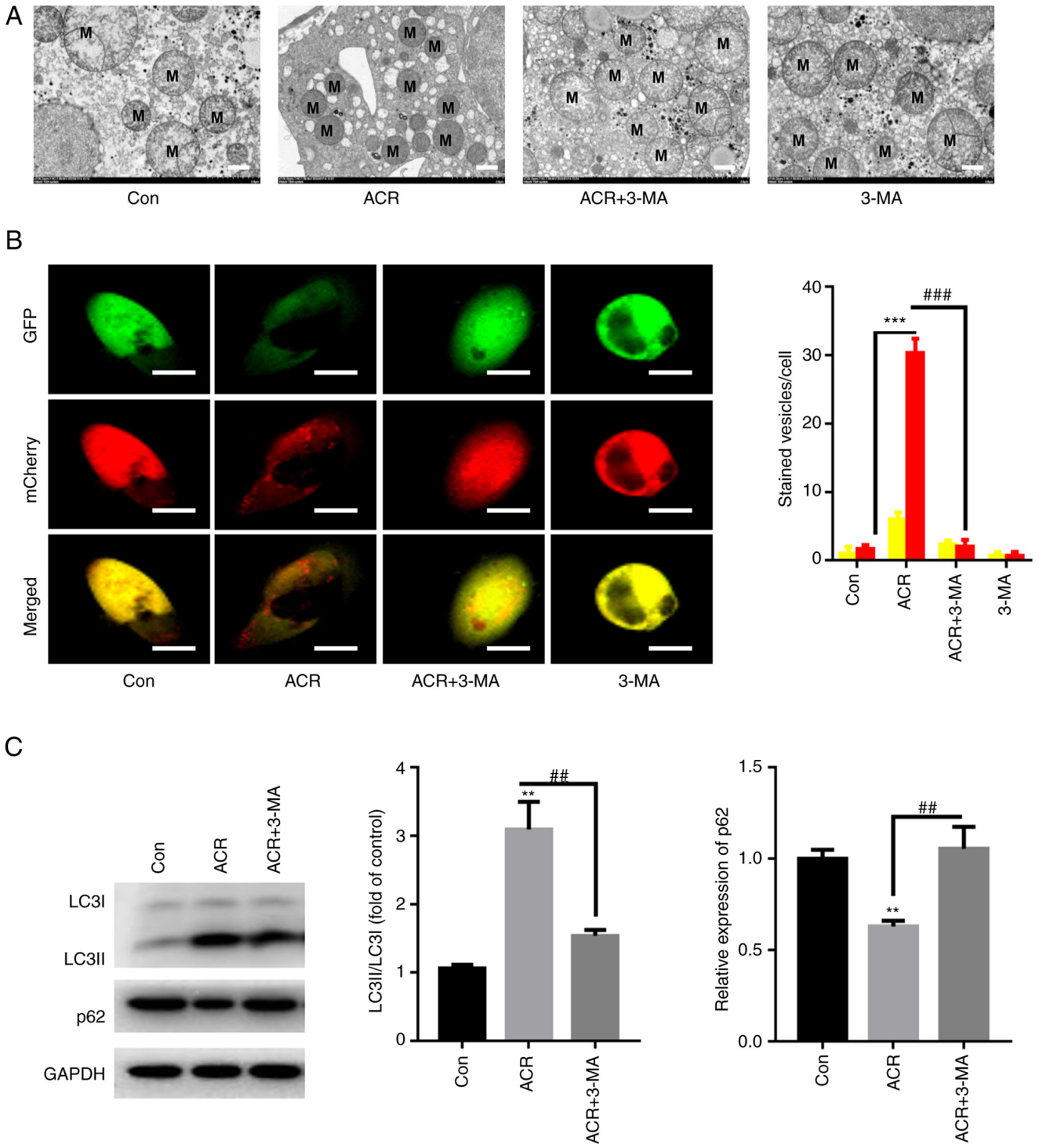

Figure 5. ACR induces autophagy in human chondrocytes. (A) Transmission electron microscopy demonstrated that ACR induced rupture of the mitochondrial membrane in human chondrocytes (magnification, x400; scale bar, 2 μm). (B) ACR increased the number of red puncta in human chondrocytes whereas preincubation with 3-MA reversed these effects (magnification, x40; scale bar, 10 μm). (C) Western blot analysis showed that ACR increased LC3II/LC3I ratio whereas it decreased sequestosome 1 expression in human chondrocytes. **P<0.01 and ***P<0.001 vs. Con. $^{\#\#}$P<0.01 and $^{\#\#\#}$P<0.001 vs. ACR. ACR, acrylamide; Con, control; p62, sequestosome 1; 3-MA, 3-methyladenine; LC, light chain; M, mitochondria.

AMPK phosphorylation is known to phosphorylate ULK1 and inhibit mTOR phosphorylation, thereby activating autophagy (35). The present data showed that ACR significantly elevated the phosphorylation levels of AMPK and ULK1 in human chondrocytes. Notably, the effect of ACR was diminished by siRNA AMPK treatment, as evidenced by the decreased lipid ROS accumulation, Fe^{2+} levels and cell autophagy. Hence, it was hypothesized that ACR activated autophagy-dependent ferroptosis by activating AMPK signaling.

However, there are limitations in the present study. First, ACR groups with different treatment doses were not considered. Secondly, a positive control group was not implemented. In the future, a positive group, such as interleukin-1β, should be included.

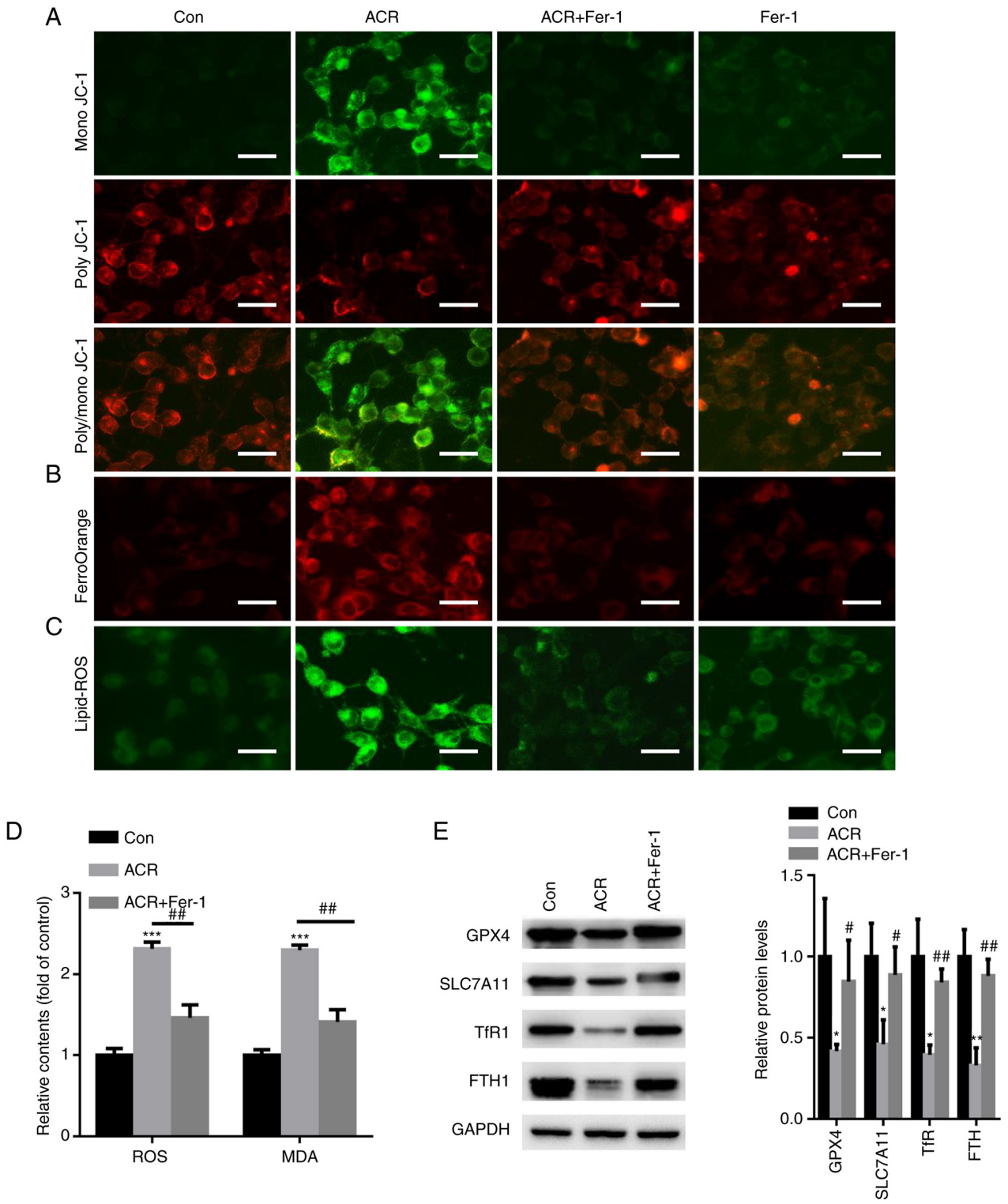

Figure 6. ACR promotes ferroptosis in human chondrocytes. (A) Cell mitochondrial membrane potential was detected in human chondrocytes treated with ACR (magnification, x20; scale bar, 20 μm). (B) FerroOrange staining showed that ACR increased intracellular Fe^{2+} levels in human chondrocytes (magnification, x20; scale bar, 20 μm). (C) C11 BODIPY fluorescent staining showed that ACR increased lipid-ROS accumulation (magnification, x20; scale bar, 20 μm). (D) Fer-1 attenuates ACR-induced upregulation of ROS and malondialdehyde content in human chondrocytes. (E) Western blot analysis demonstrated that ACR decreased expression of GPX4, SLC7A11, TfR1 and FTH1 in chondrocytes. *P<0.05 vs. Con, **P<0.01 and ***P<0.001; $^{\#}$P<0.05, $^{\#\#}$P<0.01 vs. ACR. ACR, acrylamide; Con, control; ROS, reactive oxygen species; MDA, malondialdehyde; GPX4, glutathione peroxidase 4; TfR1, transferrin receptor protein 1; SLC7A11, solute carrier family 7 member 11; FTH1, ferritin heavy chain 1; Fer-1, ferrostatin-1.

The present findings indicated that ACR inhibited cell proliferation and contributed to cell death by inducing autophagy-dependent ferroptosis and that ACR promoted autophagy by activating AMPK/ULK1/mTOR signaling in human chondrocytes. It was hypothesized that the presence of ACR in foodstuffs may increase the risk of AS and that decreasing ACR in food products is of importance.

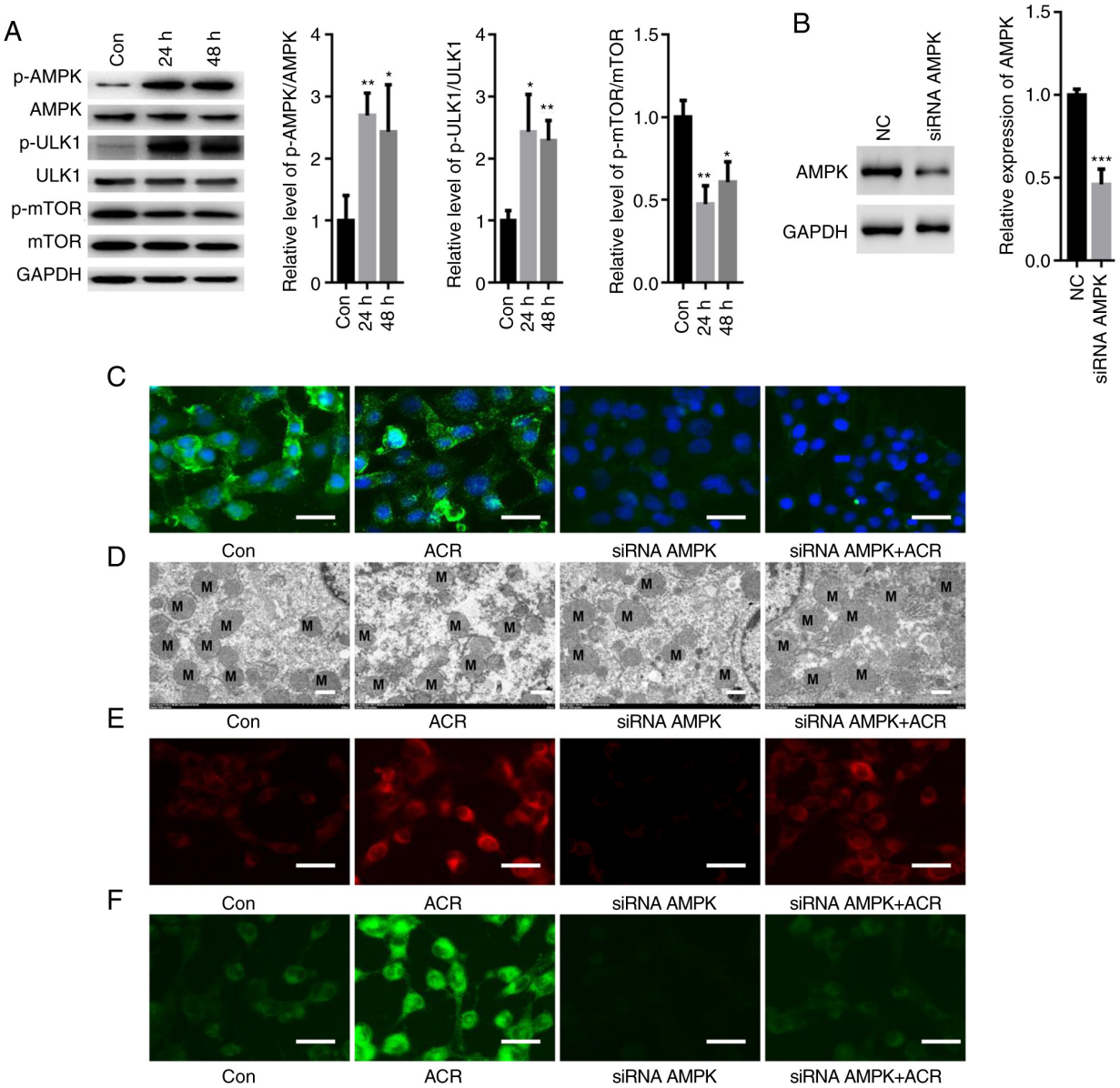

Figure 7. ACR activates AMPK/ULK1 signaling in human chondrocytes. (A) Western blot analysis showed that ACR increased phosphorylation of AMPK and ULK1 while suppressing the activation of mTOR in human chondrocytes at 24 and 48 h. (B) Western blot assay showed that transfection with siRNA-AMPK significantly suppressed expression of AMPK. (C) Immunofluorescence staining showed that siRNA AMPK significantly suppressed fluorescence density of AMPK in human chondrocytes even in the presence of ACR (magnification, x20; scale bar, 20 μm). (D) Transmission electron microscopy showed that ACR-induced mitochondrial membrane rupture was notably reversed by silencing AMPK in human chondrocytes (magnification, x400; scale bar, 2 μm). Upregulation of (E) lipid ROS and (F) Fe^{2+} was blocked by transfection with siRNA-AMPK (magnification, x20; scale bar, 20 μm). *P<0.05, **P<0.01 and ***P<0.001 vs. Con. AMPK, AMP-activated protein kinase; ACR, acrylamide; Con, control; NC, negative control; p-, phosphorylated; si, small interfering.

Acknowledgements

Not applicable.

Funding

This study was supported by the Natural Science Foundation of Shandong Province (grant no. 83562185).

Availability of data and materials

The datasets used and/or analyzed during the current study are available from the corresponding author upon reasonable request.

Authors' contributions

HW performed the experiments. ZT, SL and KX performed the western blot experiments. HW and HZ designed the experiments and analyzed the data. All authors have read and approved the final manuscript. HW and HZ confirm the authenticity of all the raw data.

Ethics approval and consent to participate

Ethics approval for commercially purchased primary human chondrocytes was obtained from the Ethics Review Committee of Zaozhuang Municipal Hospital (approval no. ZMH-2021aj32).

Patient consent for publication

Not applicable.

Competing interests

The authors declare that they have no competing interests.

References

1. Qian H, Chen R, Wang B, Yuan X, Chen S, Liu Y and Shi G: Associations of platelet count with inflammation and response to anti-TNF-α therapy in patients with ankylosing spondylitis. Front Pharmacol 11: 559593, 2020.
2. Song GG and Lee YH: Red cell distribution width, platelet-to-lymphocyte ratio, and mean platelet volume in ankylosing spondylitis and their correlations with inflammation: A meta-analysis. Mod Rheumatol 30: 894-899, 2020.
3. Steiner M, Del Mar Esteban-Ortega M, Thuissard-Vasallo I, García-Lozano I, Moriche-Carretero M, García-González AJ, Pérez-Blázquez E, Sambricio J, García-Aparicio Á, Casco-Silva BF, *et al*: Measuring choroid thickness as a marker of systemic inflammation in patients with ankylosing spondylitis. J Clin Rheumatol 27: e307-e311, 2021.
4. Chen W, Wang F, Wang J, Chen F and Chen T: The molecular mechanism of long non-coding RNA MALAT1-mediated regulation of chondrocyte pyroptosis in ankylosing spondylitis. Mol Cells 45: 365-375, 2022.
5. Yu T, Zhang J, Zhu W, Wang X, Bai Y, Feng B, Zhuang Q, Han C, Wang S, Hu Q, *et al*: Chondrogenesis mediates progression of ankylosing spondylitis through heterotopic ossification. Bone Res 9: 19, 2021.
6. Bleil J, Maier R, Hempfing A, Schlichting U, Appel H, Sieper J and Syrbe U: Histomorphologic and histomorphometric characteristics of zygapophyseal joint remodeling in ankylosing spondylitis. Arthritis Rheumatol 66: 1745-1754, 2014.
7. Kang R and Tang D: Autophagy and ferroptosis-what's the connection? Curr Pathobiol Rep 5: 153-159, 2017.
8. Park E and Chung SW: ROS-mediated autophagy increases intracellular iron levels and ferroptosis by ferritin and transferrin receptor regulation. Cell Death Dis 10: 822, 2019.
9. Hou W, Xie Y, Song X, Sun X, Lotze MT, Zeh HJ III, Kang R and Tang D: Autophagy promotes ferroptosis by degradation of ferritin. Autophagy 12: 1425-1428, 2016.
10. Li J, Liu J, Xu Y, Wu R, Chen X, Song X, Zeh H, Kang R, Klionsky DJ, Wang X and Tang D: Tumor heterogeneity in autophagy-dependent ferroptosis. Autophagy 17: 3361-3374, 2021.
11. Zhou Q, Fu X, Wang X, Wu Q, Lu Y, Shi J, Klaunig JE and Zhou S: Autophagy plays a protective role in Mn-induced toxicity in PC12 cells. Toxicology 394: 45-53, 2018.
12. Garg AD, Dudek AM, Ferreira GB, Verfaillie T, Vandenabeele P, Krysko DV, Mathieu C and Agostinis P: ROS-induced autophagy in cancer cells assists in evasion from determinants of immunogenic cell death. Autophagy 9: 1292-1307, 2013.
13. Rong T, Jia N, Wu B, Sang D and Liu B: New insights into the regulatory role of ferroptosis in ankylosing spondylitis via consensus clustering of ferroptosis-related genes and weighted gene co-expression network analysis. Genes (Basel) 13: 1373, 2022.
14. Mukhopadhyay S, Biancur DE, Parker SJ, Yamamoto K, Banh RS, Paulo JA, Mancias JD and Kimmelman AC: Autophagy is required for proper cysteine homeostasis in pancreatic cancer through regulation of SLC7A11. Proc Natl Acad Sci USA 118: e2021475118, 2021.
15. Koszucka A, Nowak A, Nowak I and Motyl I: Acrylamide in human diet, its metabolism, toxicity, inactivation and the associated European Union legal regulations in food industry. Crit Rev Food Sci Nutr 60: 1677-1692, 2020.
16. Rifai L and Saleh FA: A review on acrylamide in food: Occurrence, toxicity, and mitigation strategies. Int J Toxicol 39: 93-102, 2020.
17. Michalak J, Czarnowska-Kujawska M and Gujska E: Acrylamide and thermal-processing indexes in market-purchased food. Int J Environ Res Public Health 16: 4724, 2019.
18. Welkos S and O'Brien A: Determination of median lethal and infectious doses in animal model systems. Methods Enzymol 235: 29-39, 1994.
19. Zeng C, Pan F, Jones LA, Lim MM, Griffin EA, Sheline YI, Mintun MA, Holtzman DM and Mach RH: Evaluation of 5-ethynyl-2'-deoxyuridine staining as a sensitive and reliable method for studying cell proliferation in the adult nervous system. Brain Res 1319: 21-32, 2010.
20. Miao Y, Chen Y, Xue F, Liu K, Zhu B, Gao J, Yin J, Zhang C and Li G: Contribution of ferroptosis and GPX4's dual functions to osteoarthritis progression. EBioMedicine 76: 103847, 2022.
21. Kim J, Kundu M, Viollet B and Guan KL: AMPK and mTOR regulate autophagy through direct phosphorylation of Ulk1. Nat Cell Biol 13: 132-141, 2011.
22. Lee H, Zandkarimi F, Zhang Y, Meena JK, Kim J, Zhuang L, Tyagi S, Ma L, Westbrook TF, Steinberg GR, *et al*: Energy-stress-mediated AMPK activation inhibits ferroptosis. Nat Cell Biol 22: 225-234, 2020.
23. Tareke E, Rydberg P, Karlsson P, Eriksson S and Törnqvist M: Analysis of acrylamide, a carcinogen formed in heated foodstuffs. J Agric Food Chem 50: 4998-5006, 2002.
24. Dodić J, Pejin D, Dodić S, Popov S, Mastilović J, Popov-Raljić J and Zivanovic S: Effects of hydrophilic hydrocolloids on dough and bread performance of samples made from frozen doughs. J Food Sci 72: S235-S241, 2007.
25. Ni WJ and Leng XM: Down-regulated miR-495 can target programmed cell death 10 in ankylosing spondylitis. Mol Med 26: 50, 2020.
26. Ma C, Wen B, Zhang Q, Shao PP, Gu W, Qu K, Shi Y and Wang B: Emodin induces apoptosis and autophagy of fibroblasts obtained from patient with ankylosing spondylitis. Drug Des Devel Ther 13: 601-609, 2019.
27. Yao X, Sun K, Yu S, Luo J, Guo J, Lin J, Wang G, Guo Z, Ye Y and Guo F: Chondrocyte ferroptosis contribute to the progression of osteoarthritis. J Orthop Translat 27: 33-43, 2020.
28. Tan M, Zhang QB, Liu TH, Yang YY, Zheng JX, Zhou WJ, Xiong Q and Qing YF: Autophagy dysfunction may be involved in the pathogenesis of ankylosing spondylitis. Exp Ther Med 20: 3578-3586, 2020.
29. Garcia-Montoya L, Gul H and Emery P: Recent advances in ankylosing spondylitis: Understanding the disease and management. F1000Res 7: F1000 Faculty Rev-1512, 2018.
30. Wang Y, Luo J, Wang X, Yang B and Cui L: MicroRNA-199a-5p induced autophagy and inhibits the pathogenesis of ankylosing spondylitis by modulating the mTOR signaling via directly targeting ras homolog enriched in brain (Rheb). Cell Physiol Biochem 42: 2481-2491, 2017.
31. Qin X, Zhang J, Wang B, Xu G, Yang X, Zou Z and Yu C: Ferritinophagy is involved in the zinc oxide nanoparticles-induced ferroptosis of vascular endothelial cells. Autophagy 17: 4266-4285, 2021.
32. Liu J, Kuang F, Kroemer G, Klionsky DJ, Kang R and Tang D: Autophagy-dependent ferroptosis: Machinery and regulation. Cell Chem Biol 27: 420-435, 2020.
33. Zhang Y, Kong Y, Ma Y, Ni S, Wikerholmen T, Xi K, Zhao F, Zhao Z, Wang J, Huang B, *et al*: Loss of COPZ1 induces NCOA4 mediated autophagy and ferroptosis in glioblastoma cell lines. Oncogene 40: 1425-1439, 2021.
34. Koppula P, Zhuang L and Gan B: Cystine transporter SLC7A11/xCT in cancer: Ferroptosis, nutrient dependency, and cancer therapy. Protein Cell 12: 599-620, 2021.
35. Tang X, Ding H, Liang M, Chen X, Yan Y, Wan N, Chen Q, Zhang J and Cao J: Curcumin induces ferroptosis in non-small-cell lung cancer via activating autophagy. Thorac Cancer 12: 1219-1230, 2021.